

## Article

# Markedly Enhanced Photoluminescence of Carbon Dots Dispersed in Deuterium Oxide

Corneliu S. Stan<sup>1</sup>, Adina Coroaba<sup>2,\*</sup>, Conchi O. Ania<sup>3</sup>, Cristina Albu<sup>1</sup> and Marcel Popa<sup>1,4,\*</sup>

<sup>1</sup> Faculty of Chemical Engineering and Environmental Protection, Gh. Asachi Technical University D, Mangeron 73 Ave., 700050 Iasi, Romania; stancs@tuiasi.ro (C.S.S.)

<sup>2</sup> Centre of Advanced Research in Bionanoconjugates and Biopolymers, "Petru Poni" Institute of Macromolecular Chemistry of Romanian Academy, Grigore Ghica Voda 41A Alley, 700487 Iasi, Romania

<sup>3</sup> Conditions Extremes Materiaux: Haute Temperature et Irradiation (CEMHTI), UPR 3079, CNRS, Université d'Orléans, 45071 Orleans, France; conchi.ania@cnrs-orleans.fr

<sup>4</sup> Academy of Romanian Scientists, Ilfov Street, 050044 Bucharest, Romania

\* Correspondence: adina.coroaba@icmpp.ro (A.C.); marpopa2001@yahoo.fr (M.P.)

**Abstract:** In this work, we report some surprisingly interesting results in our pursuit to improve the photoluminescent emission of Carbon Dots (CDs) prepared from various precursors. By simply replacing the regular water with deuterium oxide (D<sub>2</sub>O) as a dispersion medium, the emission intensity and the subsequent quantum efficiency of the radiative processes could be markedly enhanced. The present study was performed on our previous reported works related to CDs; in each case, the preparation path was maintained accordingly. For each type of CD, the emission intensity and the absolute photoluminescence quantum yield (PLQY) were highly improved, with, in certain cases, more-than-doubled values being recorded and the gain in performance being easily noticeable with the naked eye even in plain daylight. For each type of CD dispersed in regular water and heavy water, respectively, the photoluminescent properties were thoroughly investigated through Steady State, lifetime, and absolute PLQY. To further elucidate the mechanism involved in the photoluminescence intensity enhancement, samples of D<sub>2</sub>O and H<sub>2</sub>O dispersed CDs were embedded in a crosslinked Poly(acrylic acid) polymer matrix. The investigations revealed the major influence of the deuterium oxide dispersion medium over the PL emission properties of the investigated CDs.



Academic Editor: Jandro L. Abot

Received: 9 December 2024

Revised: 15 January 2025

Accepted: 19 January 2025

Published: 22 January 2025

**Citation:** Stan, C.S.; Coroaba, A.;

Ania, C.O.; Albu, C.; Popa, M.

Markedly Enhanced

Photoluminescence of Carbon Dots Dispersed in Deuterium Oxide. *C* **2025**, *11*, 10. <https://doi.org/10.3390/c11010010>**Copyright:** © 2025 by the authors.

Licensee MDPI, Basel, Switzerland.

This article is an open access article distributed under the terms and conditions of the Creative Commons Attribution (CC BY) license

[\(https://creativecommons.org/licenses/by/4.0/\)](https://creativecommons.org/licenses/by/4.0/).**Keywords:** carbon nanodots; photoluminescence; deuterated mediums

## 1. Introduction

Photoluminescent Carbon Dots (CDs) are a newer established class of carbon materials which gained a lot of research interest in the last decade due to their high application potential in optoelectronic devices, sensors, medical investigations [1–3], and even food sciences [4]. One of their particular properties is the observed emission peaks dependence on the excitation wavelength, which triggered a lot of debate regarding the involved photoluminescence mechanisms. To date, the contribution of both the defect-rich,  $\pi$ -bond-conjugated, graphitic-like configuration of the carbon core and the radiative transitions arising from the surface-located functional groups is still a generally accepted open debate subject [5–7]. While the first study regarding the influence of deuterium substitution of hydrogen in naphthalene over its phosphorescence arising from triplet states is dated to the beginning of the 1960s [8], to date, there are still a limited number of studies regarding this matter. More recently, the benefit of deuterated water over the luminescent emission

was studied in a wider range of fluorescent dyes [9,10], the results being impressive since the enhancement of the recorded PL intensity varies within 30–70% range. A similar effect of increasing the fluorescent intensities induced by deuterium oxide was reported for intercalated dyes, such as fluorochromes bound to DNA [11], or in the case of liquid chromatography with fluorescence detection [12]. The presence of deuterium in various dyes, proteins, and lanthanide compounds is also able to produce a notable enhancement of their luminescent emission [13]. Also, in the pursuit of improving the performance of the OLED displays in terms of efficiency and long-term operational stability, hydrogen replacement with deuterium in TADF/AlQ/Q2AlOAr emitters was found to be highly effective in achieving these goals [14,15]. In a very recent study, CDs prepared from citric acid via a hydrothermal route were dispersed both in water and deuterium oxide, and a similar markedly increased emission was recorded. Thus, the PLQY values were doubled in case of D<sub>2</sub>O-prepared CDs. The structural analysis revealed, according to the authors, the replacement to a certain extent of hydrogen with deuterium within the CDs structure [13–16], which provide, in their view, a decisive contribution in achieving the overall emission intensity improvement. As will be further presented, our investigation does not necessarily sustain the claim regarding the significant contribution of the H to D substitution within the CDs structure to the observed emission intensity improvement. While the effective deuteration of the CDs might play a significant role in achieving better PLQY, the particular conditions provided by the D<sub>2</sub>O dispersion medium environment are, in our opinion, the main trigger of the markedly enhanced emission efficiency. In this work, CDs prepared through thermal processing of some imide precursors and argan waste were dispersed in deuterium oxide and further investigated through Steady State, lifetime, and PLQY fluorescence. For gathering more information regarding the role of D<sub>2</sub>O in achieving the recorded enhancement of photoluminescent emission, the CDs dispersions were further embedded in a crosslinked Poly(acrylic acid) polymer matrix. The reported results could bring additional evidence in the pursuit of definitive elucidation of the specific PL mechanisms of CDs and also an interesting approach for their applications in optoelectronics, sensors, and medical imaging, where an as-high-as-possible emission intensity is often required. Also, given the observed markedly enhanced PL emission in D<sub>2</sub>O medium, this study may trigger further interest in research related to deuteration and deuterated mediums.

## 2. Materials and Methods and Preparation

### 2.1. Materials

N-Hydroxyphthalimide (NHF) (97%), N-Hydroxysuccinimide (NHS), anhydrous ferric chloride (FeCl<sub>3</sub>), acrylic acid (AA), *N,N'*-Methylenebisacrylamide (MBAM), 1-Hydroxycyclohexyl phenyl ketone (HCPK), deuterium oxide (D<sub>2</sub>O), and ethanol (EtOH) were sourced from Merck Chemicals Darmstadt, Germany. Argan cake waste obtained during argan oil preparation through cold pressing was provided by a local Moroccan co-operative. Ultra-pure distilled water (Merck-Millipore-Direct Q) was used during preparation stages.

### 2.2. Methods

Freshly prepared samples were investigated through steady-state fluorescence, the emission spectra were recorded on a Horiba Fluoromax 4P spectrofluorometer (Horiba Ltd., Kyoto, Japan). In each case of pair investigation (H<sub>2</sub>O vs. D<sub>2</sub>O), the measurement parameters (entrance/exit slits and integration time) were kept unchanged. The absolute photoluminescence quantum yield (PLQY) values were recorded with the Quanta Φ integration sphere controlled by the Horiba spectrofluorometer according to the equip-

ment manufacturer's procedure using FluorEssence software (ver. 3.5.1.20) for spectral acquisition and subsequent calculations of the QY and CIE1931 parameters. Excited-states lifetimes (LT) were investigated on the same equipment with the attached Horiba Lifetime module using a 370 nm LED excitation source.

A dimensional analysis (DLS) was performed on a Malvern Panalytical Zetasizer Advance Pro Red (Malvern Panalytical Ltd., Malvern, UK). Freshly prepared and one-week-aged dispersions were investigated.

### 2.3. Preparation

Each type of CD was prepared according to experimental approach detailed in our previous works. Briefly, NHF (NHF-CDs) [17], NHS (NHS-CDs) [18], argan waste CDs (AW-CDs) [19] and NHF-Fe(III) complex (Fe-CDs) [20], were prepared by thermal processing of the respective precursors, followed by dispersion in H<sub>2</sub>O and D<sub>2</sub>O and further centrifugation, purification and dimensional selection. In case of Fe(III) doped CDs (Fe-CDs), additional steps for preparation/purification of the intermediate Fe(III)-NHF complex is required. For the embedment of the CDs in the polymer matrix the following experimental procedure was followed: in each 1.5 mL of freshly prepared NHF-CDs dispersed in D<sub>2</sub>O and H<sub>2</sub>O, respectively, 140 mmol AA and 2 mmol MBAm (as crosslinker) were dissolved under stirring, followed by the addition of 0.1 mmol of HCPK (as photoinitiator). Then, the mixture is transferred in a conveniently shaped container and further photopolymerized through exposure to a UV-A (360–370 nm) source. The photopolymerization process is fast (under 60 s), depending on the UV-A source type (in our case a 365 nm LED array was used).

## 3. Results and Discussion

### 3.1. Photoluminescence Investigation

One of the most interesting and sought after features of CDs is their PL emission, which is excitation-wavelength-dependent in most reported cases. Besides the type of precursors and the chosen preparation route, their PL emission characteristics are strongly dependent on the dispersion environment, the solvent or the polymer matrix types being key factors in terms of PL emission efficiency and location of the emission peaks [17,21]. The PL mechanism of CDs is still an open debate subject with a general opinion in favor of both contribution of the defect-rich, disordered graphitic core and the radiative transitions arising from the surface-located functional groups [6]. As mentioned in Section 1, there are several studies regarding the influence of deuteration over the emission intensity of CDs or other fluorophores where the "isotope effect" is highlighted as the main reason of the observed emission enhancement [16,22]. According to our study, there are several observations worth mentioning regarding this approach: (a) spontaneous H → D exchange might occur for a certain functional groups especially in case of organic fluorophores (-OH, NH) when solved in D<sub>2</sub>O but less probable in the case of CDs where the highly packed carbonaceous core involves bonding stability achieved through high temperature carbonization of the precursor; (b) deuteration is more likely to occur in the surface-located functional groups attached to the carbonaceous core of the CDs especially when the hydrothermal (with D<sub>2</sub>O instead of H<sub>2</sub>O as processing medium) route is used for their preparation; (c) CDs obtained through the wider spread route of direct thermal exposure (pyrolytic or not) of the precursor is less capable of sustaining a H → D exchange since the CDs are already structurally stable within the D<sub>2</sub>O dispersion medium. In this case, a preliminary stage of H → D exchange within the precursor might provide a certain level of structural deuteration of the resulting CDs. Generally, the efficiency of the radiative transitions could be markedly affected by the surroundings of the emissive species. In

aqueous dispersions, the efficiency of the radiative processes is lowered by the vicinity of the OH oscillators favoring vibrational coupling which provide an efficient non-radiative deactivation path of the excited states [23,24]. Given the configuration of the CDs with their multiple emission sites located within the carbonaceous core or in the surface-attached functional groups, it is expected that the overall efficiency of the radiative processes to be strongly affected. Switching water to deuterium oxide provides a more favorable surrounding where the non-radiative deactivation paths are markedly diminished, thus favoring the radiative relaxations through photon production. Given the particularities of D<sub>2</sub>O [25], which dissociates less than H<sub>2</sub>O, and the new vibrational conditions due to the presence of the heavier deuterium providing a better environment for the photonic processes within the CDs. Therefore, in our view and due to the investigations results detailed here, the isotope effect plays an indirect role in enhancing the PL emission by providing a more favorable environment for the radiative transitions.

### 3.1.1. Steady-State Fluorescence Investigation

For each investigated type of CD, the spectra were recorded at three excitation wavelengths (330, 350, 370 nm), with the equipment measuring parameters (entrance/exit slits, integration time, etc.) kept unchanged. In Figure 1 are presented the recorded spectra recorded for NHF-CDs dispersions in H<sub>2</sub>O and D<sub>2</sub>O, respectively, while the embedded pictures (recorded using a commonly available laboratory 370 nm UV lamp) could provide a clear view regarding the visually perceived emission intensity difference between the two samples. As could be noted, the recorded spectral intensity at any excitation wavelength is at least 2.4× higher in case of NHF-CDs dispersed in D<sub>2</sub>O, which is consistent with the visually perceived observation. In both cases, the location of the peaks remain practically unchanged irrespective of the excitation wavelength, with the most intense peaks being recorded at 370 nm excitation.

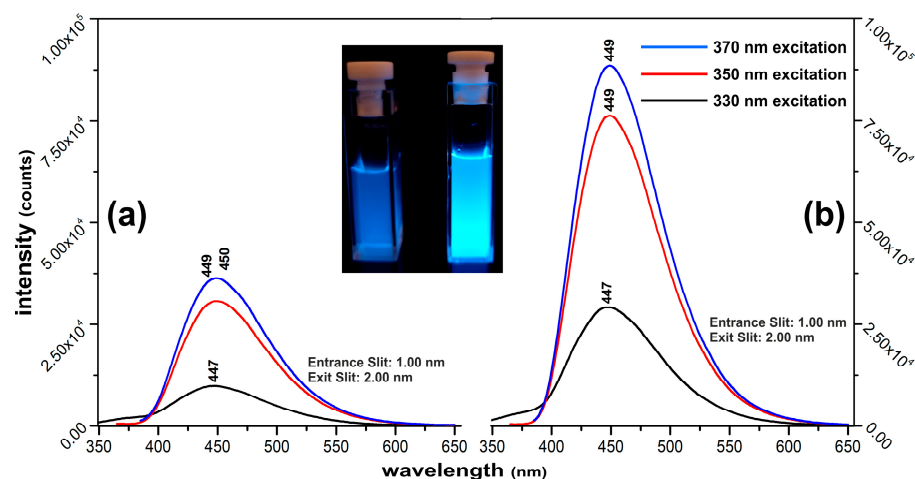


**Figure 1.** PL emission of the NHF-CDs dispersed in (a) water, (b) deuterium oxide.

In case of the NHS-CDs (Figure 2), the emission intensity enhancement in the D<sub>2</sub>O environment is still significant (both instrumental and visual) but not as impressive as observed in the previous situation. Overall, the emission intensity of this type of CDs is markedly lower compared with the NHF-CDs (please note the entrance/exit slits values) but still 1.2× higher for the NHS-CDs dispersed in D<sub>2</sub>O. The recorded emission peaks remain unchanged at 350 and 370 nm excitation, with a minor difference (414 to 417 nm) being noted at a 330 nm excitation. The maximum intensity peaks were, in both cases, recorded at 350 nm excitation.

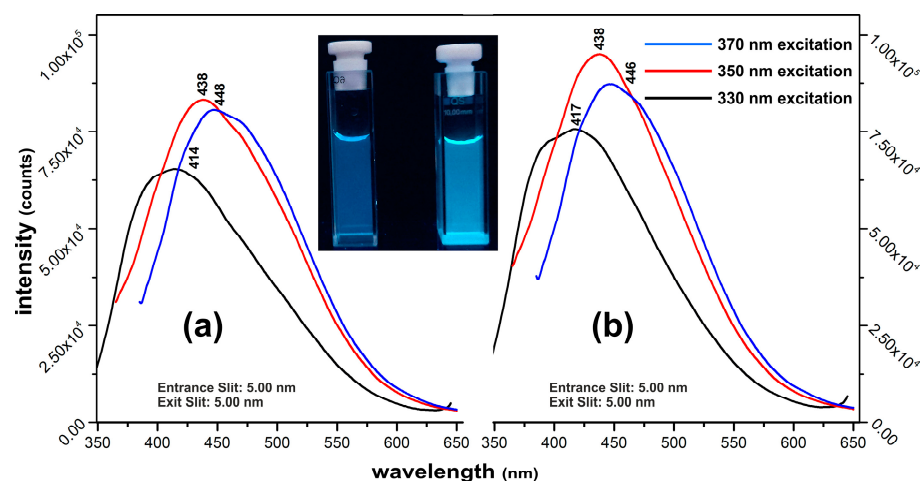


**Figure 2.** PL emission of the NHS-CDs dispersed in (a) water, (b) deuterium oxide.

The AW-CDs (Figure 3) displayed a similar behavior as the NHS-CDs, with a clearly enhanced emission recorded for the D<sub>2</sub>O dispersions. In both cases (H<sub>2</sub>O and D<sub>2</sub>O dispersions), the most intense peaks are recorded at the 370 nm excitation wavelength, their location being unchanged at the 350 nm excitation, with a slight difference (414 to 417 nm) recorded at the 330 nm and (448 to 446 nm) at the 370 nm excitation wavelengths. In all cases, the observed unchanged location of the emission peaks (in H<sub>2</sub>O and D<sub>2</sub>O dispersions) are consistent with other reported works where the emission peaks in deuterated solvents show no significant shift [6].

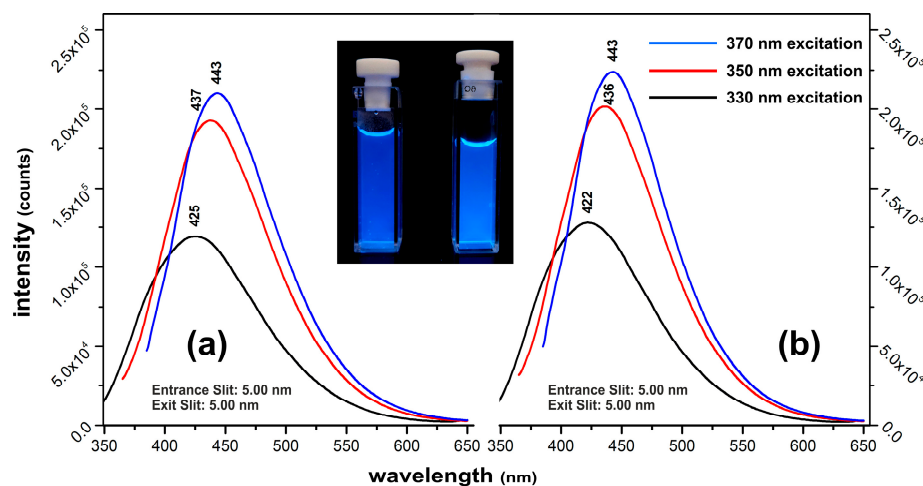


**Figure 3.** PL emission of the AW-CDs dispersed in (a) water, (b) deuterium oxide.

The green-emitting Fe(III)-doped CDs prepared by thermal processing of an Fe(III)-NHF complex also present a markedly enhanced emission when dispersed in D<sub>2</sub>O (Figure 4). As could be noted, the enhanced emission intensity is highlighted both instrumentally and visually. The recorded emission intensity is at least  $1.6\times$  higher in D<sub>2</sub>O dispersion at all investigated excitation wavelengths, the most intense emission being achieved at 350 nm excitation. Practically, there are no differences between emission peaks, the variations ( $\pm 1$  nm) could be safely attributed to the inherent measuring and/or results interpretation errors. As mentioned above, the recorded results for all four types of prepared CDs led to the conclusion that the enhancement of the PL emission intensity is rather a result of more favorable conditions achieved in the D<sub>2</sub>O dispersion environment, which provide significantly less non-radiative vibrational deactivation routes compared

with H<sub>2</sub>O dispersions. In our view, the “isotope effect” could be only indirectly used to provide a convincing insight regarding the generally observed PL intensity enhancement.

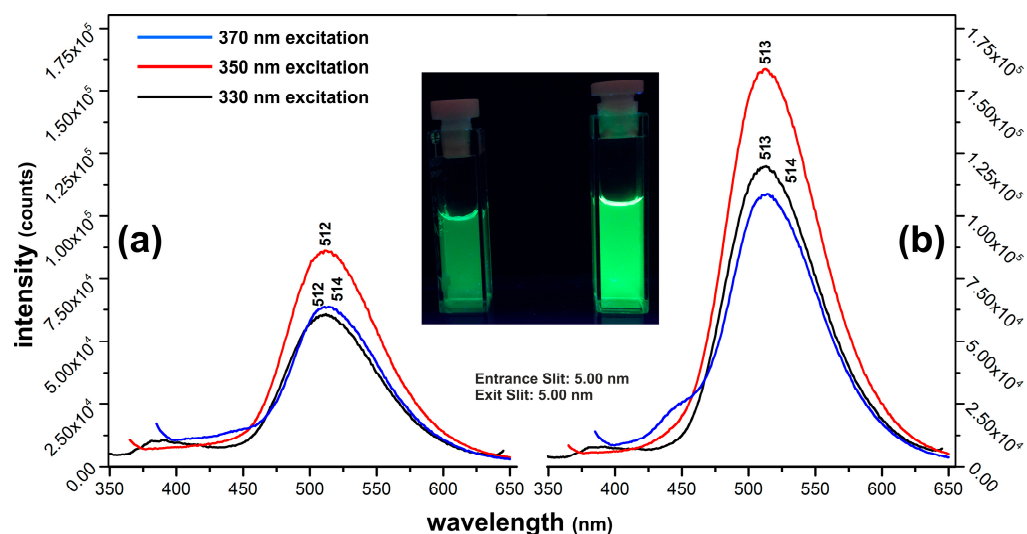


**Figure 4.** PL emission of the Fe-CDs dispersed in (a) water, (b) deuterium oxide.

To further strengthen the above-mentioned observations, we also investigated the behavior of both NHF-CDs dispersions in D<sub>2</sub>O and H<sub>2</sub>O when embedded in a polymer matrix (Section 2.3). Changing the surroundings of the NHF-CDs could be a good test of the hypothetical contribution of H → D exchange within the CDs structure. In Figure 5 are presented the observed PL intensities of the NHF-CDs/monomer/crosslinker/photoinitiator in the D<sub>2</sub>O mixture just after the commencing of the photopolymerization process (a) and post-polymerization when a solid nanocomposite of NHF-CDs trapped in the crosslinked polymer matrix is obtained (b). While within the initial 0–5 s after the UV exposure of the mixture, the characteristic blue emission of the NHF-CDs is intense, it becomes gradually fainter towards the end of the photopolymerization when the polymer matrix is completely established with the CDs trapped within. The entire process is demonstrated in the short video file (Video S1) attached to this manuscript. Due to the fast polymerization process (within a 40 s interval), the diminishing PL blue emission is clearly noticeable, most probably being a result of changing the emissive sites surrounding the conditions. At the end of the process, the initial q.ty of D<sub>2</sub>O of the mixture is mostly expelled, the crosslinked polymer matrix backbone being the new surrounding environment for the NHF-CDs.

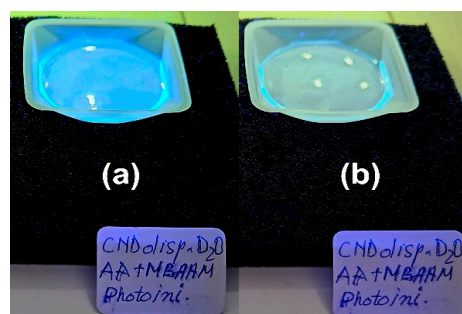


**Figure 5.** Observed PL emission intensity of the NHF-CDs/monomer/crosslinker/photoinitiator/D<sub>2</sub>O mixture (a) prior and (b) post-polymerization.

### 3.1.2. PLQY Measurements

The PLQY investigation revealed the notable enhancement of the radiative processes involved in the CDs photoluminescence. The results are included in Table 1 along with the CIE 1931 chromaticity parameters. The most impressive results were recorded in the

case of D<sub>2</sub>O-dispersed NHF-CDs, where the highest QY (70.97%) was recorded at the 350 nm excitation wavelength, the value of which is more than 2.3× higher compared with the same CDs dispersed in H<sub>2</sub>O, while at the 330 nm excitation, the QY is more than 3× higher. For the NHS-CDs, the PLQY is almost two times higher when D<sub>2</sub>O is used as a dispersion medium, a very good value (25.47%) being achieved at the 370 nm excitation. In the case of the D<sub>2</sub>O-dispersed Fe-CDs, the results are equally impressive, with the PLQY gain at the 330 nm excitation in the D<sub>2</sub>O medium being almost 2.4× higher (29.10%) compared to the same batch dispersed in H<sub>2</sub>O (12.20%). The results recorded for 350 and 370 nm excitation are also notable: 1.63× and 1.9× increased QY values in the case of the D<sub>2</sub>O-dispersed Fe-CDs. The least impressive results were recorded in the case of AW-CDs, where the highest PLQY (30.17%) was recorded at the 370 nm excitation for the batch dispersed in D<sub>2</sub>O, only a 1.27× improvement compared with the H<sub>2</sub>O dispersion (23.67%). The values recorded at 330 and 350 nm excitation are even less noticeable, the differences between the D<sub>2</sub>O and H<sub>2</sub>O batches being within the 0.3–0.84% range. The CIE 1931 chromaticity parameters revealed, in each case, minor differences between the D<sub>2</sub>O- and H<sub>2</sub>O-dispersed CDs results, which are in very good agreement with the previously discussed configuration of the emission peaks, which also revealed insignificant variations between the same batches dispersed in D<sub>2</sub>O and H<sub>2</sub>O, respectively.

**Table 1.** Recorded values for absolute PLQY and CIE 1931 chromaticity parameters.

		Absolute PLQY		
Excitation (nm)		330	350	370
CNDs NHF H <sub>2</sub> O dispersed	PLQY (%)	13.37	30.13	34.05
	abs. error (+/−)	0.028	0.066	0.086
	CIE 1931 coord.	x = 0.14588 y = 0.10874	x = 0.15215 y = 0.11844	x = 0.15235 y = 0.11802
CNDs NHF D <sub>2</sub> O dispersed	PLQY (%)	41.48	71.27	70.97
	abs. error (+/−)	0.086	0.143	0.146
	CIE 1931 coord.	x = 0.15165 y = 0.11366	x = 0.15299 y = 0.11746	x = 0.15285 y = 0.11656
CNDs NHS H <sub>2</sub> O dispersed	PLQY (%)	11.92	12.31	12.46
	abs. error (+/−)	0.041	0.048	0.07
	CIE 1931 coord.	x = 0.16148 y = 0.14843	x = 0.16749 y = 0.17764	x = 0.17203 y = 0.20566
CNDs NHS D <sub>2</sub> O dispersed	PLQY (%)	21.41	22.26	25.47
	abs. error (+/−)	0.118	0.144	0.279
	CIE 1931 coord.	x = 0.1580 y = 0.13088	x = 0.16467 y = 0.15574	x = 0.17064 y = 0.19365
CNDs Fe doped H <sub>2</sub> O dispersed	PLQY (%)	12.2	10.43	5.38
	abs. error (+/−)	0.025	0.015	0.015
	CIE 1931 coord.	x = 0.23316 y = 0.55765	x = 0.24067 y = 0.6311	x = 0.23791 y = 0.58452
CNDs Fe doped D <sub>2</sub> O dispersed	PLQY (%)	29.1	17.09	10.29
	abs. error (+/−)	0.086	0.021	0.057
	CIE 1931 coord.	x = 0.23471 y = 0.55098	x = 0.23704 y = 0.5814	x = 0.23234 y = 0.55199
CNDs Argan H <sub>2</sub> O dispersed	PLQY (%)	15.94	19.93	23.67
	abs. error (+/−)	0.04	0.059	0.102
	CIE 1931 coord.	x = 0.14839 y = 0.08361	x = 0.15448 y = 0.10221	x = 0.15723 y = 0.12234

Table 1. Cont.

		Absolute PLQY		
Excitation (nm)		330	350	370
CNDs Argan	PLQY (%)	16.24	21.77	30.17
D <sub>2</sub> O dispersed	abs. error (+/−)	0.04	0.069	0.164
	CIE 1931 coord.	x = 0.15136 y = 0.09372	x = 0.15611 y = 0.11137	x = 0.15501 y = 0.1093

Overall, the D<sub>2</sub>O dispersion medium allows for an impressive improvement in terms of efficiency of the CDs specific radiative processes compared with H<sub>2</sub>O. The PLQY improvement might vary depending on the specific structural configuration of different types of CDs prepared from a certain precursor. According to our observations, a initially higher PLQY of a certain type of CDs dispersed in H<sub>2</sub>O will produce an even higher gain in PL efficiency when D<sub>2</sub>O is used. An already good PLQY is most probably due to the richness of the emissive sites within the CDs structure, which will highly benefit from a dispersion medium, which is less prone to provide non-radiative paths leading to premature deactivation of the excited states.

### 3.1.3. Fluorescence Lifetime (LT) Measurements

In Figure 6A–H are illustrated the typical time-resolved fluorescence decay profiles (in Figure S1A–H the residuals of the fluorescence decay fitting), while in Table 2 are presented the relevant decay characteristics. To accurately model the fluorescence decay behavior, we employed a single exponential decay model or a multi-exponential decay model, depending on the sample behavior (Equation (1)) [9,26,27]:

$$I(t) = \sum_{i=1}^n a_i \cdot \exp\left(\frac{-t}{\tau_i}\right) \quad (1)$$

where  $I(t)$  is the fluorescence intensity, and  $a_i$  corresponds to the amplitude of each component  $i$ , which reflects the relative contribution of that specific decay process. Each component is characterized by a unique fluorescence lifetime  $\tau_i$ , and the sum of all amplitudes is normalized to 1 ( $\sum a_i = 1$ ), ensuring that the model represents the entirety of the observed decay. To further understand the contribution of each lifetime component, we calculated the fractional concentration, ( $f_i$ ) of each decay time, which quantifies the proportion of fluorescence attributable to each lifetime (Equation (2)):

$$f_i = \frac{a_i \tau_i}{\sum_{j=1}^n a_j \tau_j} \quad (2)$$

The sum of  $f_i$  values is also normalized to 1 ( $\sum_{i=1}^n f_i = 1$ ), indicating that the calculated fractions account for the total observed fluorescence. The average lifetime ( $\langle\tau\rangle$ ) was given by this Equation (3):

$$\langle\tau\rangle = f_1 \tau_1 + f_2 \tau_2 + f_3 \tau_3 \quad (3)$$

In the present study, the fluorescence decay in water was best described by a three-exponential model. However, the same three-exponential model also applied to two of the deuterated samples, NHS-CDs and AW-CDs. Interestingly, for the NHF-CDs and Fe-CDs samples in deuterated solvent, a single-exponential decay was observed. Additionally, we found that the D<sub>2</sub>O dispersion medium increased the average lifetimes compared to the H<sub>2</sub>O dispersed samples, a phenomenon reported by others in the literature as well [9,27].

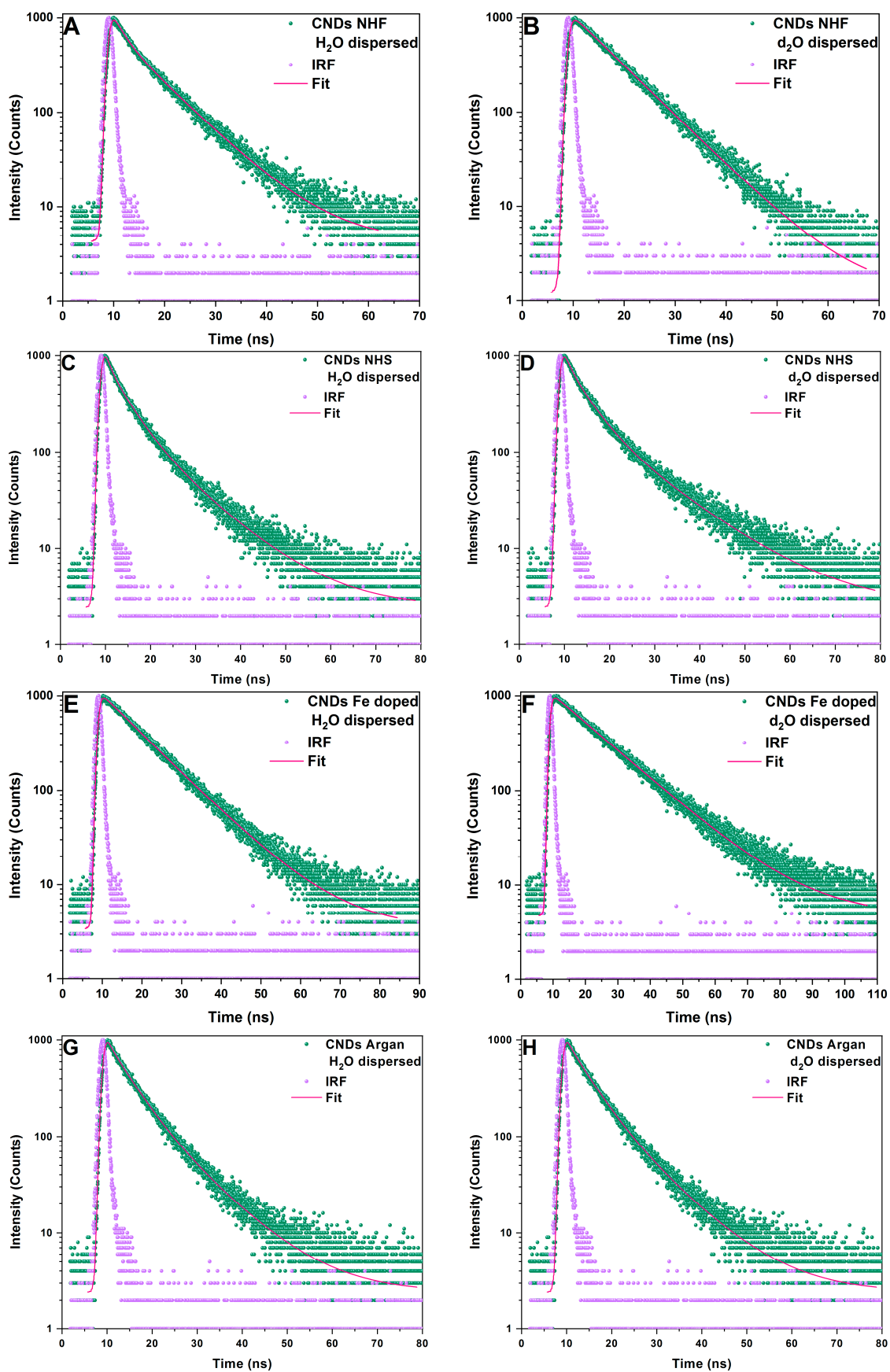


**Figure 6.** The typical time-resolved fluorescence decay profiles of the (A) NHF-CDs/H<sub>2</sub>O, (B) NHF-CDs D<sub>2</sub>O, (C) NHS-CDs/H<sub>2</sub>O, (D) NHS-CDs/D<sub>2</sub>O, (E) Fe-CDs/H<sub>2</sub>O, (F) Fe-CDs/D<sub>2</sub>O, (G) AW-CDs/H<sub>2</sub>O, and (H) AW-CDs/D<sub>2</sub>O samples.

**Table 2.** Absolute PLQY at  $\lambda_{\text{ex}} = 370$  nm, radiative and non-radiative decay rate constants, and fluorescence lifetimes of the analyzed samples.

Sample Code	$\Phi$ (%)	$k_r$ * ( $\text{ns}^{-1}$ )	$k_{nr}$ * ( $\text{ns}^{-1}$ )	$\tau_1$ (ns)	$a_1$ (%)	$f_1$	$\tau_2$ (ns)	$a_2$ (%)	$f_2$	$\tau_3$ (ns)	$a_3$ (%)	$f_3$	$\chi^2$	$\langle\tau\rangle$ (ns)
NHF-CDs H <sub>2</sub> O dispersed	34.05	0.042	0.082	8.38	81.43	0.952	2.09	16.33	0.048	0.11	2.24	0.000	1.04	8.07
NHF-CDs D <sub>2</sub> O dispersed	70.97	0.086	0.035	8.22	100.00	1.000	-	-	-	-	-	-	1.09	8.22
NHS-CDs H <sub>2</sub> O dispersed	12.46	0.014	0.101	10.68	44.22	0.698	4.20	46.42	0.289	0.95	9.36	0.013	1.11	8.68
NHS-CDs D <sub>2</sub> O dispersed	25.47	0.024	0.071	12.72	47.40	0.744	4.39	45.47	0.246	1.04	7.13	0.009	1.13	10.56
NHS-CDs H <sub>2</sub> O dispersed	5.38	0.005	0.089	12.98	17.83	0.222	9.99	81.00	0.778	0.09	1.17	0.000	1.10	10.66
Fe-CDs D <sub>2</sub> O dispersed	10.29	0.007	0.061	14.65	100.00	1.000	-	-	-	-	-	-	1.07	14.65
AW-CDs H <sub>2</sub> O dispersed	23.67	0.029	0.094	9.85	46.75	0.673	4.49	49.43	0.324	0.47	3.82	0.003	1.11	8.09
AW-CDs D <sub>2</sub> O dispersed	30.17	0.028	0.066	12.88	47.32	0.713	5.09	46.97	0.280	1.12	5.17	0.007	1.14	10.62

$\Phi$  = fluorescence quantum yield,  $\tau_{1,2,3}$  = fluorescence lifetimes,  $a_{1,2,3}$  = amplitude of the components,  $f_{1,2,3}$  = fractional concentrations,  $\langle\tau\rangle$  = average fluorescence lifetimes,  $k_r$  = radiative rate constants,  $k_{nr}$  = non-radiative rate constants. \* calculated for the  $\Phi$  at  $\lambda_{\text{ex}} = 370$  nm.

Additionally, to provide insight into the decay mechanisms, we derived both radiative ( $k_r$ ) and non-radiative ( $k_{nr}$ ) decay constants (Table 2) from nanosecond lifetime measurements and quantum yields using the following equations:

$$k_r = \frac{\Phi}{\langle\tau\rangle} \quad (4)$$

$$k_{nr} = \frac{1 - \Phi}{\langle\tau\rangle} \quad (5)$$

Generally,  $k_{nr}$  is higher than  $k_r$  for each sample, indicating that non-radiative decay processes are more prominent, which may contribute to the observed differences in fluorescence behavior in H<sub>2</sub>O and D<sub>2</sub>O. Furthermore, the influence of the deuterated solvent led to a decrease in the non-radiative decay constant ( $k_{nr}$ ) and an increase in the radiative decay constant ( $k_r$ ). This shift in decay pathways aligns with the observed increase in quantum yield when the samples are dispersed in deuterated solvent compared to regular water. The reduction in  $k_{nr}$  suggests that the non-radiative relaxation processes, such as vibrational relaxation and other energy-dissipating mechanisms, are less prominent in deuterated solvent. This reduction could be attributed to the isotope effect, where deuterium atoms, with their greater mass, decrease vibrational energy dissipation, effectively reducing non-radiative losses. At the same time, the increase in  $k_r$  indicates that the radiative decay pathway (fluorescence emission) becomes more favorable in the presence of deuterated solvent, contributing to the enhanced quantum yield. These changes suggest that deuterated solvents can shift the balance between radiative and non-radiative decay processes, enhancing fluorescence efficiency by promoting radiative decay while suppressing non-radiative pathways [28]. Therefore, the LT investigation results are in very good agreement with PLQY and Steady-State fluorescence investigations, sustaining very well our opinion that the “isotope effect” induced by the D<sub>2</sub>O presence plays an indirect role in enhancing the PL emission by providing a more favorable environment for the radiative transitions.

### 3.2. Characterization of the D<sub>2</sub>O Dispersed CDs

As stated above, the experimental procedure for the preparation of each type of investigated CDs was kept unchanged, as detailed in our previous reported works [14–17], where an in-depth morpho-structural investigation was performed and discussed. Since the only difference consists of the final dispersion medium (D<sub>2</sub>O), the investigations presented in this work were focused on the morphological aspects which could provide new information. Therefore, the DLS (dimensional analysis) was performed for each type of CDs dispersed in D<sub>2</sub>O.

#### Dimensional (DLS) Investigation

Freshly prepared samples of each type of CDs dispersed in D<sub>2</sub>O were investigated. Also, for the evaluation of longer-term stability of the dispersions, same samples were investigated again after 1 week. In Figure 7a–d are presented the dimensional distributions for each type of CDs dispersed in D<sub>2</sub>O, freshly prepared and after 1 week of aging.

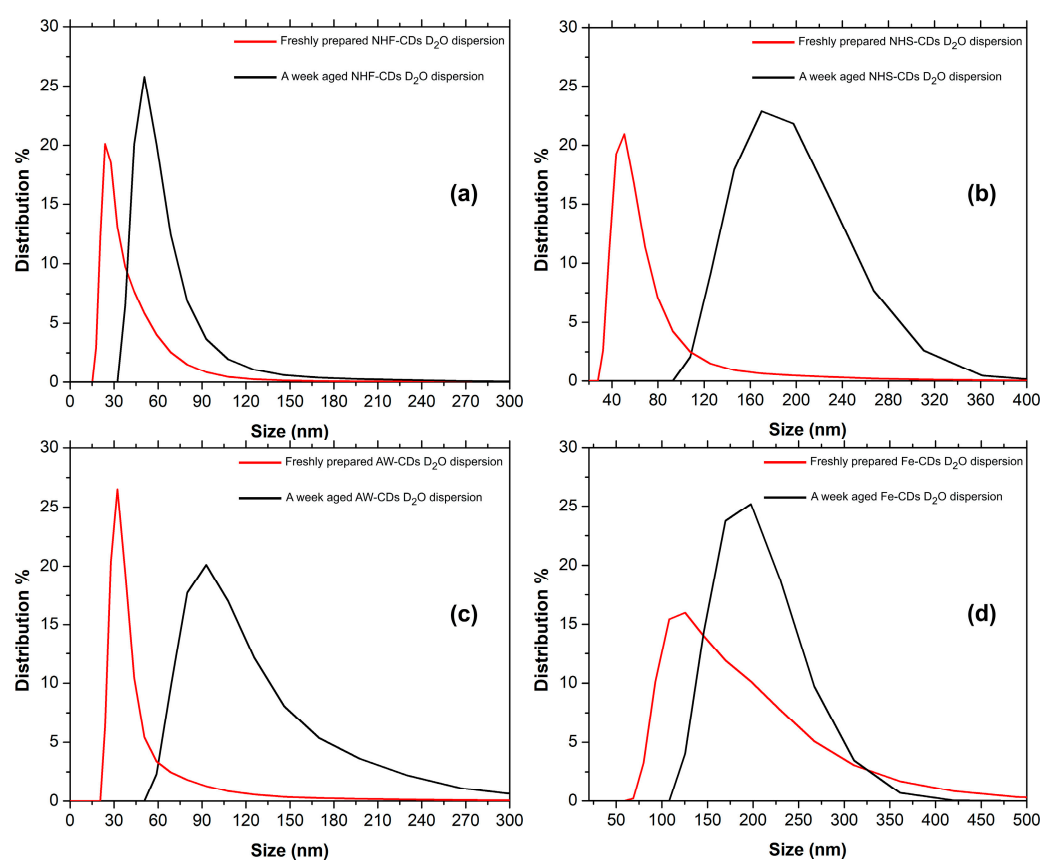


**Figure 7.** Dimensional distribution of freshly prepared/1 week aged of (a) NHF-CDs, (b) NHS-CDs, (c) AW-CDs, and (d) Fe-CDs dispersed in D<sub>2</sub>O.

All the prepared samples present, as expected, an agglomeration tendency which was observed irrespective of the type of solvent used as dispersion medium. The freshly prepared NHF-CDs/D<sub>2</sub>O dispersion size distribution is mainly situated within 30–90 nm range. As demonstrated in our previous works, CDs present a clusterization tendency which became even more noticeable in case of the aged dispersion where the size distribution migrates within 40–140 nm range. In case of NHS-CDs, the freshly prepared dispersion presents a narrower size distribution (40–120 nm) compared with the aged dispersion where a broad 120–320 nm distribution was observed most probably due to an even more clusterization tendency. This behavior is almost the same in the case of AW-CDs where the freshly prepared dispersion presents a narrow distribution (25–90 nm), which becomes

significantly broader for the aged dispersion (60–250 nm). The Fe-CDs/D<sub>2</sub>O dispersion behaves differently compared with the rest of the investigated samples, with an initial broad distribution (60–400 nm), which also remain large but slightly translated to higher dimensional range (100–400 nm). This particular behavior could be a result of iron presence within the CDs structure. Overall, the stability of the dispersions is slightly better compared with the same CDs types but dispersed in water.

Interestingly, in the case of NHF-CDs, AW-CDs, and Fe-CDs dispersions, the PL intensity remained unchanged after 1 week, no notable differences being noticed both visually and instrumentally, which might additionally sustain the key role of the dispersion medium in achieving a better emissive intensity. The aged NHS-CDs/D<sub>2</sub>O dispersion presents a slightly fainter emission intensity. Compared with samples of same CDs type dispersed in water, the PL emission is markedly better preserved.

#### 4. Conclusions

The photoluminescence (PL) properties of several types of Carbon Dots (CDs) dispersed in deuterium oxide were thoroughly investigated. Through simple replacement of the commonly used aqueous dispersion medium with D<sub>2</sub>O, the CDs prepared from various precursors are able to achieve an impressive enhancement of their PL emission intensity. In the present work, four types of CDs were prepared, the emission intensity being markedly enhanced in each case. The recorded PL quantum yield (QY) was found to increase at least  $1.27\times$  to  $2.3\times$  compared with the same CDs batches dispersed in H<sub>2</sub>O, an impressive 70.97% QY being achieved in the most favorable case. The isotope effect over the PL properties of fluorophores (including CDs) is a less investigated research topic with relatively scarce reported works. Unlike many of the reported studies which hypothesize that the observed PL intensity enhancement is a result of the isotope effect induced by spontaneous H → D exchange within the CDs structure, our investigation supports an alternative mechanism where the isotope effect might be indirectly involved. In our view, switching H<sub>2</sub>O to D<sub>2</sub>O as the dispersion medium allows for the ability to provide a more favorable environment, which diminishes the non-radiative deactivation paths, thus favoring the radiative relaxations through photon production. Given the particularities of D<sub>2</sub>O, which dissociates less than H<sub>2</sub>O, and the new vibrational conditions due to the presence of the heavier deuterium in the surroundings of the emissive sites, a better environment for the photonic processes is provided within the CDs.

**Supplementary Materials:** The following supporting information can be downloaded at <https://www.mdpi.com/article/10.3390/c11010010/s1>: Figure S1: Recorded Lifetime residuals, Video S1.

**Author Contributions:** Conceptualization, C.S.S., C.O.A. and M.P.; methodology, C.S.S., A.C. and C.O.A.; investigation, C.S.S. and A.C.; writing—original draft preparation, C.S.S. and A.C.; experimental, C.S.S. and C.A.; writing—review and editing, C.S.S. and C.O.A. All authors have read and agreed to the published version of the manuscript.

**Funding:** This work was supported by a grant from the Romanian National Authority for Scientific Research and Innovation UEFISCDI, project: ERANET 293/2022-COFUND-LEAP-RE-NANOSOLARCELL. The authors thank the financial support of the LEAP-RE program (Long-Term Joint EUAU Research and Innovation Partnership on Renewable Energy; grant NANOSOLARCELLS).

**Data Availability Statement:** The data presented in this study are available upon request from the corresponding author.

**Conflicts of Interest:** The authors declare no conflicts of interest.

## References

1. Ozyurt, D.; Al Kobaisi, M.; Hocking, R.K.; Fox, B. Properties, synthesis, and applications of carbon dots: A review. *Carbon Trends* **2023**, *12*, 100276. [[CrossRef](#)]
2. Etefa, H.F.; Tessema, A.A.; Dejene, F.B. Carbon Dots for Future Prospects: Synthesis, Characterizations and Recent Applications: A Review (2019–2023). *C* **2024**, *10*, 60. [[CrossRef](#)]
3. Ullah, M.; Awan, U.A.; Ali, H.; Wahab, A.; Khan, S.U.; Naeem, M.; Ruslin, M.; Mustopa, A.Z.; Hasan, N. Carbon Dots: New Rising Stars in the Carbon Family for Diagnosis and Biomedical Applications. *J. Nanotheranostics* **2025**, *6*, 1. [[CrossRef](#)]
4. Majid, A.; Ahmad, K.; Tan, L.; Niaz, W.; Na, W.; Huiru, L.; Wang, J. The Advanced Role of Carbon Quantum Dots in Nano-Food Science: Applications, Bibliographic Analysis, Safety Concerns, and Perspectives. *C* **2025**, *11*, 1. [[CrossRef](#)]
5. Ai, L.; Yang, Y.; Wang, B.; Chang, J.; Tang, Z.; Yang, B.; Lu, S. Insights into photoluminescence mechanisms of carbon dots: Advances and perspectives. *Sci. Bull.* **2021**, *66*, 839–856. [[CrossRef](#)]
6. Wang, B.; Lu, S. The light of carbon dots: From mechanism to applications. *Matter* **2022**, *5*, 110–149. [[CrossRef](#)]
7. Carbonaro, C.M.; Corpino, R.; Salis, M.; Mocci, F.; Thakkar, S.V.; Olla, C.; Ricci, P.C. On the Emission Properties of Carbon Dots: Reviewing Data and Discussing Models. *C* **2019**, *5*, 60. [[CrossRef](#)]
8. Hutchison, C.A.; Mangum, B.W. Effect of deuterium substitution on the lifetime of the phosphorescent triplet state of naphthalene. *J. Chem. Phys.* **1960**, *32*, 1261–1262. [[CrossRef](#)]
9. Kučera, J.; Peš, O.; Janovič, T.; Hofr, C.; Kubinyiová, L.; Tóth, J.; Káňa, Š.; Táborský, P. Enhancement of luminescence signal by deuterated water—Practical implications. *Sens. Actuators B Chem.* **2022**, *352*, 131029. [[CrossRef](#)]
10. Gamage, R.; Smith, B. Fluorescence imaging using deep-red Indocyanine Blue (ICB) a complementary partner for near infrared Indocyanine Green (ICG). *Chem. Biomed. Imaging* **2024**, *2*, 384–397. [[CrossRef](#)] [[PubMed](#)]
11. Sailer, B.L.; Nastasi, A.J.; Valdez, J.G.; Steinkamp, J.A.; Crissman, H.A. Differential Effects of Deuterium Oxide on the Fluorescence Lifetimes and Intensities of Dyes with Different Modes of Binding to DNA. *J. Histochem. Cytochem.* **1997**, *45*, 165–175. [[CrossRef](#)]
12. Taborsky, P.; Kucera, J.; Jurica, J.; Pes, O. Heavy water enhancement of fluorescence signal in reversed-phase liquid chromatography. *J. Chromatogr. B* **2018**, *1092*, 7–14. [[CrossRef](#)] [[PubMed](#)]
13. Filer, C.N. Luminescence enhancement by deuterium. *J. Label. Compd. Radiopharm.* **2023**, *66*, 372–383. [[CrossRef](#)]
14. Tong, C.C.; Hwang, K.C. Enhancement of OLED Efficiencies and High-Voltage Stabilities of Light-Emitting Materials by Deuteration. *J. Phys. Chem. C* **2007**, *111*, 3490–3494. [[CrossRef](#)]
15. Jung, S.; Cheung, W.L.; Li, S.; Wang, M.; Li, W.; Wang, C.; Song, X.; Wei, G.; Song, Q.; Chen, S.S.; et al. Enhancing operational stability of OLEDs based on subatomic modified thermally activated delayed fluorescence compounds. *Nat. Commun.* **2023**, *14*, 6481.
16. Yao, Z.; Wen, X.; Hong, X.; Tao, R.; Yin, F.; Cao, S.; Yan, J.; Wang, K.; Wang, J. Deuteration-Induced Energy Level Structure Reconstruction of Carbon Dots for Enhancing Photoluminescence. *Adv. Sci.* **2024**, *11*, 2308523. [[CrossRef](#)] [[PubMed](#)]
17. Stan, C.S.; Horlescu, P.; Ursu, L.E.; Popa, M.; Albu, C. Facile preparation of highly luminescent composites by polymer embedding of carbon dots derived from N-hydroxyphthalimide. *J. Mater. Sci.* **2017**, *52*, 185–196. [[CrossRef](#)]
18. Stan, C.S.; Albu, C.; Coroaba, A.; Popa, M.; Sutiman, D. One step synthesis of fluorescent Carbon Dots through pyrolysis of N-hydroxysuccinimide. *J. Mater. Chem. C* **2015**, *3*, 789–795. [[CrossRef](#)]
19. Stan, C.S.; Elouakassi, N.; Albu, C.; Ania, C.O.; Coroaba, A.; Ursu, L.E.; Popa, M.; Kaddami, H.; Almaggoussi, A. Photoluminescence of Argan-Waste-Derived Carbon Nanodots Embedded in Polymer Matrices. *Nanomaterials* **2024**, *14*, 83. [[CrossRef](#)] [[PubMed](#)]
20. Stan, C.S.; Coroaba, A.; Ursu, E.L.; Secula, M.S.; Simionescu, B.C. Fe(III) doped carbon nanodots with intense green photoluminescence and dispersion medium dependent emission. *Sci. Rep.* **2019**, *9*, 18893. [[CrossRef](#)] [[PubMed](#)]
21. Papaioannou, N.; Marinovic, A.; Yoshizawa, N.; Goode, A.E.; Fay, M.; Khlobystov, A.; Titirici, M.M.; Sapelkin, A. Structure and solvents effects on the optical properties of sugar-derived carbon nanodots. *Sci. Rep.* **2018**, *8*, 6559. [[CrossRef](#)]
22. Ma, Z.; Zhang, L.; Cui, Z.; Ai, X. Improving the Luminescence and Stability of Carbon-Centered Radicals by Kinetic Isotope Effect. *Molecules* **2023**, *28*, 4805. [[CrossRef](#)] [[PubMed](#)]
23. Dobretsov, G.E.; Syrejschikova, T.I.; Smolina, N.V. On mechanisms of fluorescence quenching by water. *Biophysics* **2014**, *59*, 183–188. [[CrossRef](#)]
24. Maillard, J.; Klehs, K.; Rumble, C.; Vauthey, E.; Heilemann, M.; Fürstenberg, A. Universal quenching of common fluorescent probes by water and alcohols. *Chem. Sci.* **2021**, *12*, 1352–1362. [[CrossRef](#)] [[PubMed](#)]
25. Kumar, S.; Hoshino, M.; Kerkeni, B.; Kerkeni, B.; García, G.; Limão-Vieira, P. Isotope Effect in D2O Negative Ion Formation in Electron Transfer Experiments: DO–D Bond Dissociation Energy. *J. Phys. Chem. Lett.* **2023**, *14*, 5362–5369. [[CrossRef](#)] [[PubMed](#)]
26. Coroaba, A.; Al-Matarneh, C.; Vasiliu, T.; Ibanescu, S.-A.; Zonda, R.; Esanu, I.; Isac, D.-L.; Pinteala, M. Revealing the supramolecular interactions of the bis(azopyrenyl) dibenzo-18-crown-6-ether system. *J. Mol. Liq.* **2023**, *374*, 121298. [[CrossRef](#)]

- 
27. Magde, D.; Wong, R.; Seybold, P.G. Fluorescence Quantum Yields and Their Relation to Lifetimes of Rhodamine 6G and Fluorescein in Nine Solvents: Improved Absolute Standards for Quantum Yields. *Photochem. Photobiol.* **2002**, *75*, 327–334. [[CrossRef](#)] [[PubMed](#)]
  28. Lakowicz, J.R. *Principles of Fluorescence Spectroscopy*, 3rd ed.; Lakowicz, J.R., Ed.; Springer Science & Business Media: New York, NY, USA, 2007.

**Disclaimer/Publisher's Note:** The statements, opinions and data contained in all publications are solely those of the individual author(s) and contributor(s) and not of MDPI and/or the editor(s). MDPI and/or the editor(s) disclaim responsibility for any injury to people or property resulting from any ideas, methods, instructions or products referred to in the content.